

Comparative proteomic analysis of the mitochondria of menstrual stem cells and ovarian cancer cells

XIUHUI CHEN^{1*}, WEN ZHONG^{1*}, YUE CHANG², TIEFANG SONG¹,
BOTONG LIU¹, XIANCHAO KONG¹ and QINGFEI KONG³

¹Department of Obstetrics and Gynecology, The Second Affiliated Hospital of Harbin Medical University, Harbin, Heilongjiang 150086; ²Department of Obstetrics and Gynecology, Beijing Friendship Hospital, Capital Medical University, Beijing 100050; ³Department of Neurobiology, Harbin Medical University, Harbin, Heilongjiang 150086, P.R. China

Received May 1, 2022; Accepted November 10, 2022

DOI: 10.3892/etm.2023.11798

Abstract. Mitochondrial transplantation is a popular field of research in cell-free therapy. Menstrual stem cells (MenSCs) are potential donor cells for provision of foreign mitochondria. The present study aimed to investigate the potential effects of MenSC-derived mitochondria on ovarian cancer from the perspective of protein expression profiling. MenSCs were harvested from menstrual blood. The mitochondria were isolated from MenSCs and ovarian cancer cell line SKOV3. A label-free mitochondria proteomics and analysis were performed by comparing the protein expression in mitochondria of MenSCs and SKOV3 cells. The differentially expressed proteins with fold-change >2 were analyzed by Gene Ontology, Kyoto Encyclopedia of Genes and Genomes pathway and protein domain enrichment, protein interaction networks and parallel reaction monitoring (PRM) analysis. In total, 592 proteins that were found to have increased expression in the mitochondria of MenSCs were analyzed. Functional enrichment analysis revealed these proteins were enriched in metabolism-associated pathway entries including 'oxidative phosphorylation' (OXPHOS) pathway. PRM analysis confirmed that four of 6 candidate proteins in the OXPHOS pathway showed similar increasing trends. The protein domain enrichment analysis showed that domains such as 'thioredoxin

domain' were significantly enriched. Based on these findings, it was hypothesized that mitochondria from MenSCs have the potential to enhance progression of ovarian cancer likely mediated by the enrichment of OXPHOS-associated metabolic pathways.

Introduction

Menstrual stem cells (MenSCs) are a novel population of cells derived from human menstrual blood that possess typical characteristics (self-renewal and multilineage differentiation potential) of mesenchymal SCs (MSCs) (1). As an alternative source of MSCs, MenSCs have competitive advantages such as non-invasive acquisition procedure and high proliferation capability (2). However, they also share similar safety concerns to MSCs, such as unpredictable pro-tumor effects and tissue entrapment (3). Cell-free therapies using cellular components, which exhibit the benefits of cellular therapy while avoiding the disadvantages, have been drawing increasing attention (4,5). Previous studies have demonstrated the therapeutic value of SC-derived exosomes for various diseases (6,7), particularly cancer treatment (8). Mitochondria are a popular target in cell-free therapy. Besides being the primary energy supplier, mitochondria also work as carriers of enriched genetic cargo participating in multiple cellular functions, such as cellular stress responses, including apoptosis and autophagy (9,10).

Alteration of energy metabolism in cancer cells was first shown by Otto Warburg (11). In addition to the dominant aerobic glycolysis, mitochondrial oxidative phosphorylation (OXPHOS) is also hypothesized to serve a key role in the metabolic mode of cancer cells (12,13). Mutations in mitochondria have been found in various tumors. For example, variants in mitochondrial biogenesis genes have been shown to influence the epithelial ovarian cancer risk (14). Previous research has revealed that the transplantation of mitochondria from different sources has adverse effects on different tumors. For example, the transfer of MSC-derived mitochondria supports tumor progression by enhancing proliferation and invasion of breast cancer and glioblastoma cells (15,16). By contrast, transplantation of mitochondria from normal human astrocytes inhibits malignant proliferation of human glioma cells (17). However, to the best of our knowledge, no studies

Correspondence to: Dr Xianchao Kong, Department of Obstetrics and Gynecology, The Second Affiliated Hospital of Harbin Medical University, 246 Xuefu Road, Harbin, Heilongjiang 150086, P.R. China
E-mail: 28607248@qq.com

Professor Qingfei Kong, Department of Neurobiology, Harbin Medical University, 157 Baojian Road, Harbin, Heilongjiang 150086, P.R. China
E-mail: 821833588@qq.com

*Contributed equally

Key words: energy metabolism, menstrual stem cell, mitochondria transplantation, oxidative phosphorylation, proteomics

have reported the effects of MenSC-derived mitochondria on cancer.

Ovarian cancer is the most lethal gynecological cancer, with a worldwide mortality rate of 1.9% (18). Molecular evidence suggests dysregulation in mitochondria associated with biogenesis, morphology, dynamics and apoptosis is involved in carcinogenesis of ovarian cancer (19). Thus, the defective mitochondria may be a potential therapeutic target. To the best of our knowledge, however, there are no previous studies on the transfer of SC-derived mitochondria to ovarian cancer. In the present study, the possible effects of MenSC-derived mitochondria on ovarian cancer were investigated from the perspective of protein expression profiling. Human ovarian carcinoma cell line SKOV3, isolated from the ascites of a patient with ovarian cancer, is typically used for *in vitro* and *in vivo* research of ovarian cancer (20). By comparing the proteome of mitochondria from MenSCs and SKOV3 cells, it was hypothesized that OXPHOS-related metabolic pathways may serve a key role in enhancement of tumor progression after mitochondrial transplantation.

Materials and methods

Ethics approval and consent to participate. The research proposal for human menstrual blood collection was approved by the Ethical Committee of The Second Affiliated Hospital of Harbin Medical University (approval no. KY2018-105). Participants signed informed consent.

Menstrual blood collection. Volunteers were from The Second Affiliated Hospital of Harbin Medical University, Harbin, Heilongjiang Province, China from January 2020 to December 2020. Donors were selected based on the following criteria: i) 20-30 years old; ii) no sexual history; iii) no history of infectious diseases; iv) regular menstrual cycles and v) normal vaginal discharge. The research proposal for human menstrual blood collection was approved by the Ethical Committee of The Second Affiliated Hospital of Harbin Medical University (approval no. KY2018-105). Participants signed informed consent. In total, 10 females were enrolled (mean age 23.4, median age, 24). In total, 5 ml menstrual blood was collected and transferred into a collection tube containing 0.1 ml penicillin/streptomycin (P/S) and 0.1 ml EDTA-Na₂ (Sigma-Aldrich; Merck KGaA) in 5 ml PBS.

Cell isolation and culture. Mononuclear cells were isolated from the collected menstrual blood by Ficoll-Paque (Sigma-Aldrich; Merck KGaA) density gradient centrifugation according to the manufacturer's protocols. The cells were cultured in a T-25 flask containing DMEM/F-12 (Invitrogen; Thermo Fisher Scientific, Inc.) supplemented with 1% P/S and 10% FBS (Invitrogen; Thermo Fisher Scientific, Inc.), at 37°C, 5%CO₂. The medium was replaced with the complete medium the next day. Once cells reached 80-90% confluence, the adherent cells were trypsinized, resuspended [wash cells twice with 3 ml PBS; add 500 µl of trypsin digestion solution (0.25%) for 3-4 min gently shake the flask to dislodge the adherent cells from the flask. Add equal volume of culture medium to terminate digestion, collect cell suspension, discard the supernatant, add culture medium to prepare cell suspension]

and cultured at a density of 1.5x10⁵ cells in a T-25 flask. The cells were passaged twice/week. 3-5 passage cells were used as indicated for all experiments. Human ovarian cancer cell line SKOV3 was obtained from Procell Life Science & Technology Co., Ltd. SKOV3 cells were maintained in DMEM (Invitrogen; Thermo Fisher Scientific, Inc.) supplemented with 10% FBS (Invitrogen; Thermo Fisher Scientific, Inc.), 100 U/ml penicillin and 100 mg/ml streptomycin. Cultures were incubated at 37°C in a humidified atmosphere containing 5% CO₂. The morphology of cultured cells was examined under a phase contrast microscope (40X magnification) (AX 70; Olympus, Japan).

Mitochondrial isolation. The mitochondria were extracted by a mitochondrial isolation kit (Abkine, KTP4003, China). Briefly, MenSCs or ovarian cancer cells were homogenized by 70 strokes using a Dounce Tissue Grinder in isolation buffer A plus protease inhibitor cocktail. Cell extracts were collected into equal volumes of isolation buffer C with buffer A. Cell debris and nuclei were removed by centrifugation at 700 x g for 10 min, 4°C, and mitochondrial fractions were collected by centrifugation at 3,000 x g for 15 min, 4°C.

Flow cytometric analysis. MenSCs or MenSC-derived mitochondria were stained and labeled with anti-human fluorophore-conjugated antibodies for CD73-FITC (BioLegend, Inc.; Cat# 344015), CD90-FITC (BioLegend, Inc. Cat#328107), CD34-FITC (BioLegend, Inc. Cat# 343503), CD45-FITC (BioLegend, Inc. Cat# 304005), CD63-PE (BioLegend, Inc. Cat# 353003) and CD29-FITC (eBioscience; Thermo Fisher Scientific, Inc. Cat# 11029942) and detected by flow cytometric analysis. Briefly, trypsinized cells or mitochondria were washed then re-suspended in ice-cold PBS containing 1% BSA (Invitrogen; Thermo Fisher Scientific, Inc.). Fluorophore-conjugated antibodies were added at concentrations recommended by the manufacturer's protocols (95 µl staining buffer, 5 µl fluorophore-conjugated antibodies) and incubated in the dark for 30 min, 25°C. The cells or mitochondria were washed twice in staining buffer (eBioscience, Thermo Fisher Scientific, Inc.) and analyzed under a flow cytometer (LSR Fortessa; BD Biosciences). Data analysis was performed using FlowJo (BD Biosciences. v.7.6.5).

Protein extraction and trypsin digestion. Protein was extracted from mitochondria in ice-cold lysis buffer [8 M urea, 2 mM EDTA, 10 mM Dithiothreitol (Sigma, Japan) and 1% Protease Inhibitor Cocktail III, Calbiochem, Germany] using a high-intensity ultrasonic processor (Ningbo Scientz Biotechnology Co., Ltd.) on ice. In total, 200 µg protein in solution (0.1% formic acid, 2% acetonitrile/in water) was used for each group to run liquid chromatography tandem mass spectrometry (LC-MS/MS) analysis. After removing the debris, protein was precipitated with cold 15% trichloroacetic acid for 2 h at -20°C. Following centrifugation at 12,000 g at 4°C for 10 min, the remaining precipitate was washed with cold acetone three times. The protein was dissolved in a buffer at pH 8.0 comprising 8 M urea and 100 mM Tetraethylammonium bromide (TEAB). For digestion, protein solution was reduced with 5 mM dithiothreitol for 30 min at 56°C and alkylated with 11 mM iodoacetamide for 15 min at

room temperature in darkness. The protein sample was diluted by adding 100 mM TEAB to urea concentration <2 M. Finally, trypsin was added at 1:50 trypsin-to-protein mass ratio for the first digestion overnight and 1:100 trypsin-to-protein mass ratio for a second 4 h digestion. The pooling of individual samples is a cost-effective approach for proteomic studies. Therefore, 10 samples with equal amounts of protein from volunteers were mixed to obtain 3 pooled samples (21).

LC-MS/MS analysis (4D label-free). 4D label-free is the new generation of quantitative proteomics. With mobility as the fourth latitude added to 3D label-free quantification, sensitivity and quality of the detection are improved. Relative protein quantification is achieved by comparing the number of identified MS/MS spectra of a sample's proteolytic peptides (22). The tryptic peptides were dissolved in solvent A (0.1% formic acid in water) and directly loaded onto a home-made reversed-phase analytical column. Peptides were separated with a gradient from 4 to 6% solvent B (0.1% formic acid in acetonitrile) in 2 min, 6 to 24% for 68 min, 24 to 32% in 14 min and climbing to 80% in 3 min, then holding at 80% for 3 min, all at a constant flow rate of 300 nL/min on a nanoElute high-performance LC system (Bruker Corporation). The peptides were subjected to Capillary source followed by the timsTOF Pro (Bruker Daltonics) mass spectrometry. The electrospray voltage was 1.60 kV. Precursors and fragments were analyzed at the TOF detector, with a MS/MS scan range from 100 to 1,700 m/z. The timsTOF Pro was operated in parallel accumulation serial fragmentation (PASEF) mode. Precursors with charge states 0-5 were selected for fragmentation and 10 PASEF-MS/MS scans were acquired/cycle. Associated parameters are set to: ionization mode positive, and we use nano-ESI (CaptiveSpray), no nebulizer; Dry Gas: 3 l/min; Dry Temp: 180°C. The dynamic exclusion was set to 30 sec.

Database search. The resulting MS/MS data were processed using Maxquant (Max-Planck-Institute of Biochemistry, v.1.6.6.0). Tandem mass spectra were searched against the Uniprot human database (20,600 sequences, accessed 03/2021) concatenated with a reverse decoy database (maxquant.org/, SETTING PARAMETERS: Database is Homosapiens9606SP20191115) Trypsin/P was specified as a cleavage enzyme allowing up to 2 missing cleavages. The mass tolerance for precursor ions was set as 40 parts/million in both first and main search and the mass tolerance for fragment ions was set as 0.04 Da. Carbamidomethyl on cysteine was specified as a fixed modification. Acetylation on protein N-terminal and oxidation on methionine were specified as variable modifications. Peptide and protein false discovery rate were adjusted to <1%.

Bioinformatics annotation analysis. Gene Ontology (GO) annotation and enrichment analysis were derived from the UniProt-GOA database (ebi.ac.uk/interpro/). If some identified proteins were not annotated, InterProScan (ebi.ac.uk/. v.5.14-53.0) was used to annotate GO function based on protein sequence alignment method. InterProScan was applied to predict the domain functional descriptions of the differentially expressed proteins. WoLF PSORT (wolfsort.hgc.jp/. NAKAI Lab.) and iLoc-Animal

(<http://www.jci-bioinfo.cn/iLoc-Animal>) were used to predict subcellular localization.

Protein-protein interaction (PPI) analysis. PPI networks and pathways were assessed by STRING (cn.string-db.org/. v.11.5) and Kyoto Encyclopedia of Genes and Genomes (KEGG, genome.jp/kaas-bin/kaas_main) database, respectively.

GO annotation. GO annotation proteomics was derived from the UniProt-GOA database (ebi.ac.uk/GOA/). Firstly, identified protein IDs were converted to UniProt IDs that were mapped to GO IDs by protein ID. If identified proteins were not annotated by the UniProt-GOA database, InterProScan software [InterProScan (<https://www.ebi.ac.uk/>. v.5.14-53.0)] was used to annotate protein GO function based on the protein sequence alignment method. Proteins were classified by GO annotation based on three categories: i) biological process; ii) cellular component and iii) molecular function.

Clusters of Orthologous Groups of proteins. COG, Orthologs refer to proteins evolved from vertical pedigrees (speciation) from different species and typically retain the same function as the original protein. COG is divided into two categories; one is prokaryotic and the other is eukaryotic. Prokaryotes are called COG databases; eukaryotes are called KOG databases. We performed COG/KOG functional classification statistics for differentially expressed proteins by database alignment analysis (ncbi.nlm.nih.gov/COG/).

Functional enrichment analysis. For each GO category, a two-tailed Fisher's exact test was employed to test enrichment of the differentially expressed protein against all identified proteins. GO with corrected $P < 0.05$ was considered to indicate statistical significance. The KEGG database was used to identify enriched pathways by two-tailed Fisher's exact test t . A pathway with corrected $P < 0.05$ was considered to indicate statistical significance. These pathways were classified into hierarchical categories (Metabolism, Genetic Information Processing, Environmental Information Processing, Cellular Processes, Organismal Systems, Human Diseases and Drug Development) according to the KEGG website. For protein domain enrichment analysis, the InterPro database was searched and a two-tailed Fisher's exact test was employed to compare enrichment of the differentially expressed protein. GO plot package (v.0.4) was employed for plotting GO or pathway annotation and abundance (<https://cran.r-project.org/web/packages/networkD3/>).

Enrichment-based clustering. For further hierarchical clustering based on differentially expressed protein functional classification (such as GO, domain, pathway), categories obtained following enrichment along with their P-values were filtered for those categories that were least enriched in one of the clusters with $P < 0.05$. This filtered P-value matrix was transformed by the function $x = -\log_{10}(P)$. Finally, these values were z-transformed for each functional category. The z-scores were then clustered by one-way hierarchical clustering (Euclidean distance, average linkage clustering) in Genesis (Genesis2000, v.9.1). Cluster membership was visualized by a heat map using the heatmap.2 function from the gplots R package (cran.r-project.org/web/packages/cluster/, v.2.0.3).

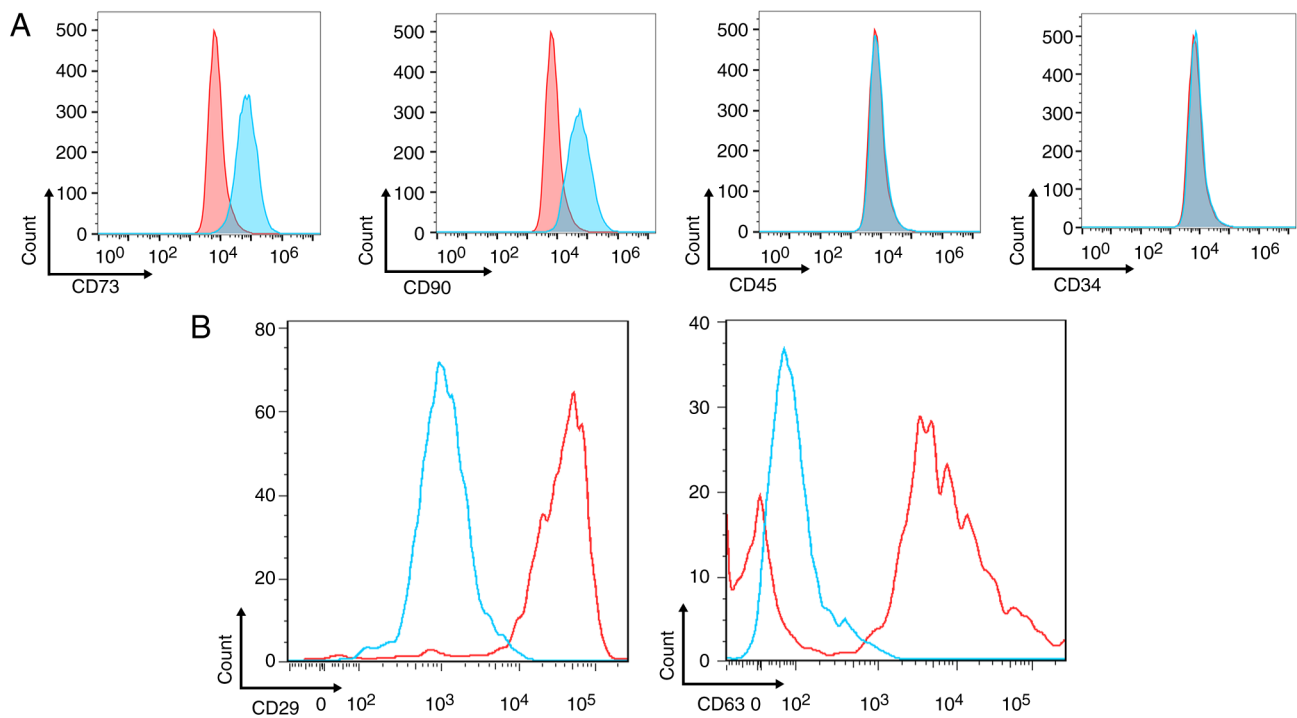


Figure 1. Characterization of MenSCs and MenSC-derived mitochondria by flow cytometry. (A) Mesenchymal stem cell markers CD73 and CD90 were positively expressed and hematopoietic stem cell markers CD34 and CD45 were negatively expressed in MenSCs. (B) Mitochondrial markers CD63 and CD29 were positively expressed in MenSC-derived mitochondria. MenSC, menstrual stem cell.

Parallel reaction monitoring (PRM) analysis. PRM is a targeted quantitative MS approach, generating high resolution precursor measurements and full scan MS/MS data (23). The target proteins suitable for PRM validation were decided by factors such as the unique sequence coverage, intensity and MS/MS count. PRM MS analysis was performed using MS/MS in Q Exactive™ Plus (Thermo Fisher Scientific, Inc.). Sample processing and performance of PRM analysis was performed by Jingjie PTM BioLab Co., Inc. LC parameters, electrospray voltage, scan range and Orbitrap resolution were the same as for the 4D label-free method. Automatic gain control was set at 3×10^6 for full MS and 1×10^5 for MS/MS. The maximum Ion Trap was set at 20 msec for full MS and was automated for MS/MS. The isolation window for MS/MS was set at 2.0 m/z. After quantitative information was normalized by the heavy isotope-labeled peptide, a relative quantitative analysis, based on three biological replicates, was performed on the target peptides.

Results

Isolation and characterization of MenSCs and mitochondria. Adherent cells showed a fibroblast-like short spindle-shaped morphology after 9-12 day primary culture and were confirmed to express surface markers similar to MSCs (expression of characteristic stem cell phenotypes, such as CD44, CD73, CD90, CD146, but not hematopoietic stem cell phenotypes CD34, CD45, CD14, CD11b); CD73 and CD90 were positively expressed and CD34 and CD45 were negatively expressed (Fig. 1A). The mitochondria were extracted from MenSCs and SKOV3 cells. Flow cytometry identified that mitochondria markers CD63 and CD29 were positively expressed (Fig. 1B).

Differentially expressed protein analysis. By LC-MS/MS, a quantitative analysis of the global proteome in mitochondria of MenSCs and SKOV3 cells was performed. In total, 5,597 proteins were identified, of which 3,856 proteins were quantified. Proteins that displayed fold-change in expression >2 were analyzed further. Compared with the mitochondria of SKOV3 cells, 592 proteins showed increased expression in mitochondria of MenSCs, while 583 proteins showed decreased expression (Fig. 2A). GO functional annotation was performed to classify candidate proteins into three categories according to their respective level 2 GO terms: i) biological process; ii) cellular component and iii) molecular function (Fig. 2B). In the category of biological process, metabolic process is the important and predominant biological process, with 727 proteins being involved.

Subcellular localization of differentially expressed proteins and functional classification. The cells of eukaryotic organisms are divided into functionally distinct membrane-bound compartments (24). The subcellular localization of differentially expressed proteins was characterized. The largest subcellular localization categories of proteins that showed increased expression were 'cytoplasm' (23.82%), 'mitochondria' (18.07%) and 'plasma membrane' (17.91%; Fig. 2C). The largest subcellular localization categories of proteins that showed decreased expression were 'cytoplasm' (41.51%), 'nucleus' (27.62%) and 'plasma membrane' (8.58%; Fig. S1). The percentage of mitochondrial proteins with increased expression was higher than those with decreased expression (18.07 vs. 7.89%). COG/EuKaryotic Orthologous Groups (COG/KOG) functional classification was performed by database alignment analysis (Fig. 2D). Most upregulated

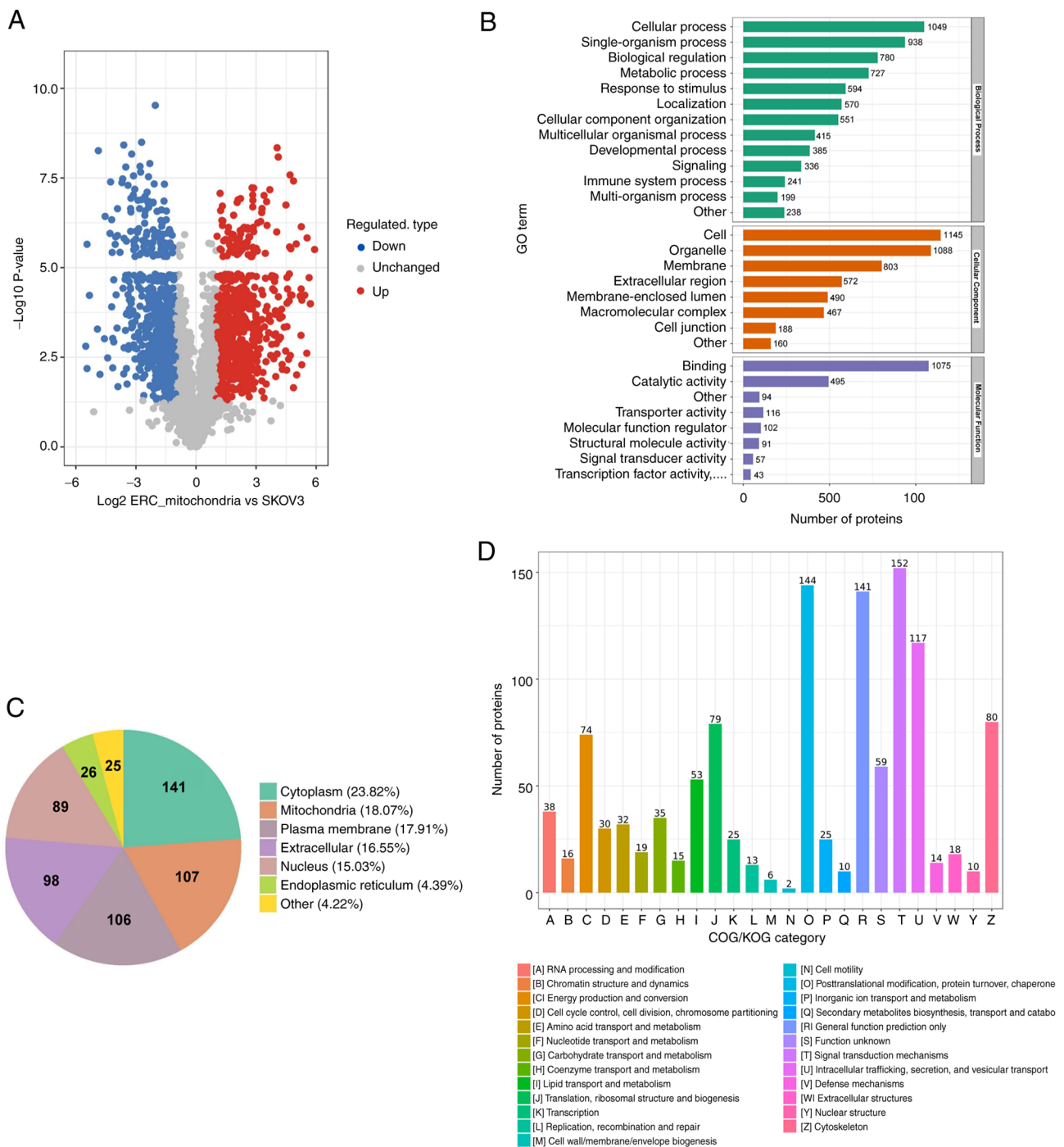


Figure 2. Basic analysis of differentially expressed proteins from 4D label-free proteomics. (A) Summary of the number of proteins identified and quantified illustrated by volcano plot. In total, 592 proteins with increased expression and 583 proteins with decreased expression were identified. (B) GO term level 2 classification of differentially expressed proteins. (C) Key areas in which proteins with increased expression were localized were 'cytoplasm' (23.82%), 'mitochondria' (18.07%) and 'plasma membrane' (17.91%). (D) COG/KOG categories indicated that functions of proteins with increased expression were most frequently classified as 'signal transduction mechanism', 'post-translational modification', protein turnover, chaperone', 'general function prediction only' and 'energy production and conversion'. MenSC-Mito, menstrual stem cell-derived mitochondria; GO, Gene Ontology; COG/KOG, Cluster of Orthologous Groups/EuKaryotic Orthologous Groups.

proteins were classified as 'signal transduction mechanism', 'post-translational modification', 'protein turnover, chaperone', 'general function prediction only' and 'energy production and conversion'.

Functional enrichment analysis of differentially expressed proteins. GO, KEGG pathway and protein domain analysis

were performed to determine functional classification of the differentially expressed proteins.

GO functional enrichment analysis revealed the most enriched functions in differentially expressed mitochondrial proteins in the three GO enrichment classification categories (Fig. 3). In proteins that showed increased expression, the top three enriched functions in each classification were

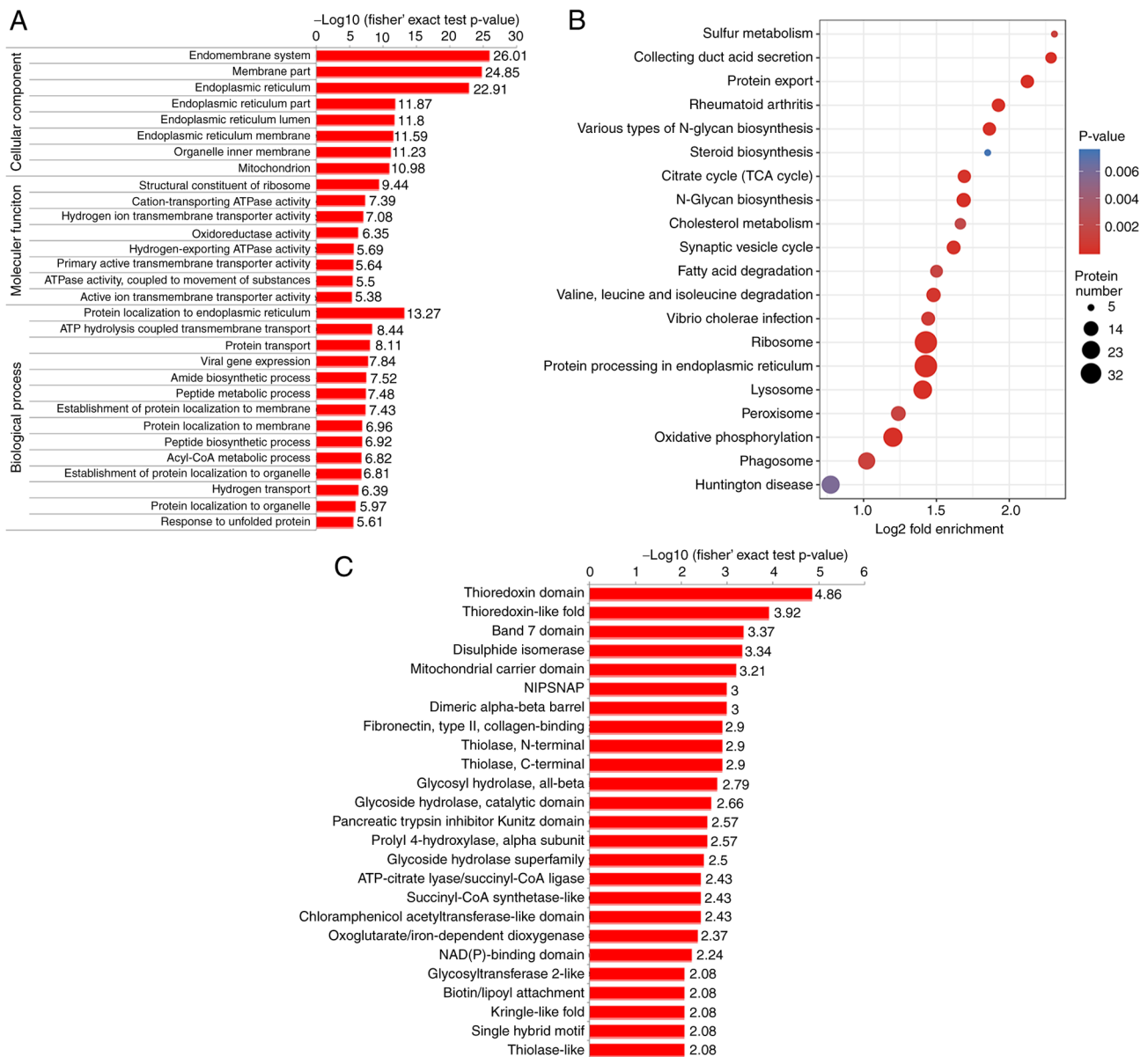


Figure 3. Functional enrichment analysis of proteins with increased expression. (A) Gene Ontology enrichment analysis of biological process, cellular component and molecular function. (B) Kyoto Encyclopedia of Genes and Genomes pathway enrichment analysis. (C) Protein domain enrichment analysis.

'endomembrane system', 'membrane part' and 'endoplasmic reticulum'; 'structural constituent of ribosome', 'cation-transporting ATPase activity' and 'hydrogen ion transmembrane transporter activity' and 'protein localization to endoplasmic reticulum', 'ATP hydrolysis coupled transmembrane transport' and 'protein transport' (Fig. 3A). Enrichment analysis of proteins that showed decreased expression is shown in Fig. S2A. In proteins that showed decreased expression, the top three enriched functions in each classification were 'extracellular exosome', 'extracellular organelle' and 'extracellular vesicle'; 'cell adhesion molecule binding', 'cadherin binding' and 'nucleotide binding'; 'actin cytoskeleton organization', 'neutrophil mediated immunity' and 'myeloid leukocyte activation'.

KEGG pathway enrichment analysis showed that proteins that showed increased expression were enriched in 25 pathway entries; functions associated with 'protein processing in

endoplasmic reticulum', 'ribosome', 'lysosome', 'protein export' and 'oxidative phosphorylation' were most significantly enriched (Fig. 3B). The components and cascades of the OXPHOS pathway are shown in Fig. 4. The expression levels of NADH:ubiquinone oxidoreductase subunit S5 (NDUFS5), NDUFS6, succinate dehydrogenase complex iron sulfur subunit B (SDHB), cytochrome c oxidase subunit 5B (COX5B), cytochrome c oxidase subunit 4 (COX4), NDUFA7 and NDUFB4 were significantly increased in MenSC-derived mitochondria and these proteins were identified in the OXPHOS signaling pathway by KEGG pathway analysis (Fig. 4). This pathway has functions in energy metabolism and driving ATP synthesis, which promote cell proliferation. The pathways in which proteins that displayed decreased expression were primarily enriched are shown in Fig S2B, such as 'tight junction', 'regulation of actin cytoskeleton', 'adherens junction' and 'central carbon metabolism in cancer';

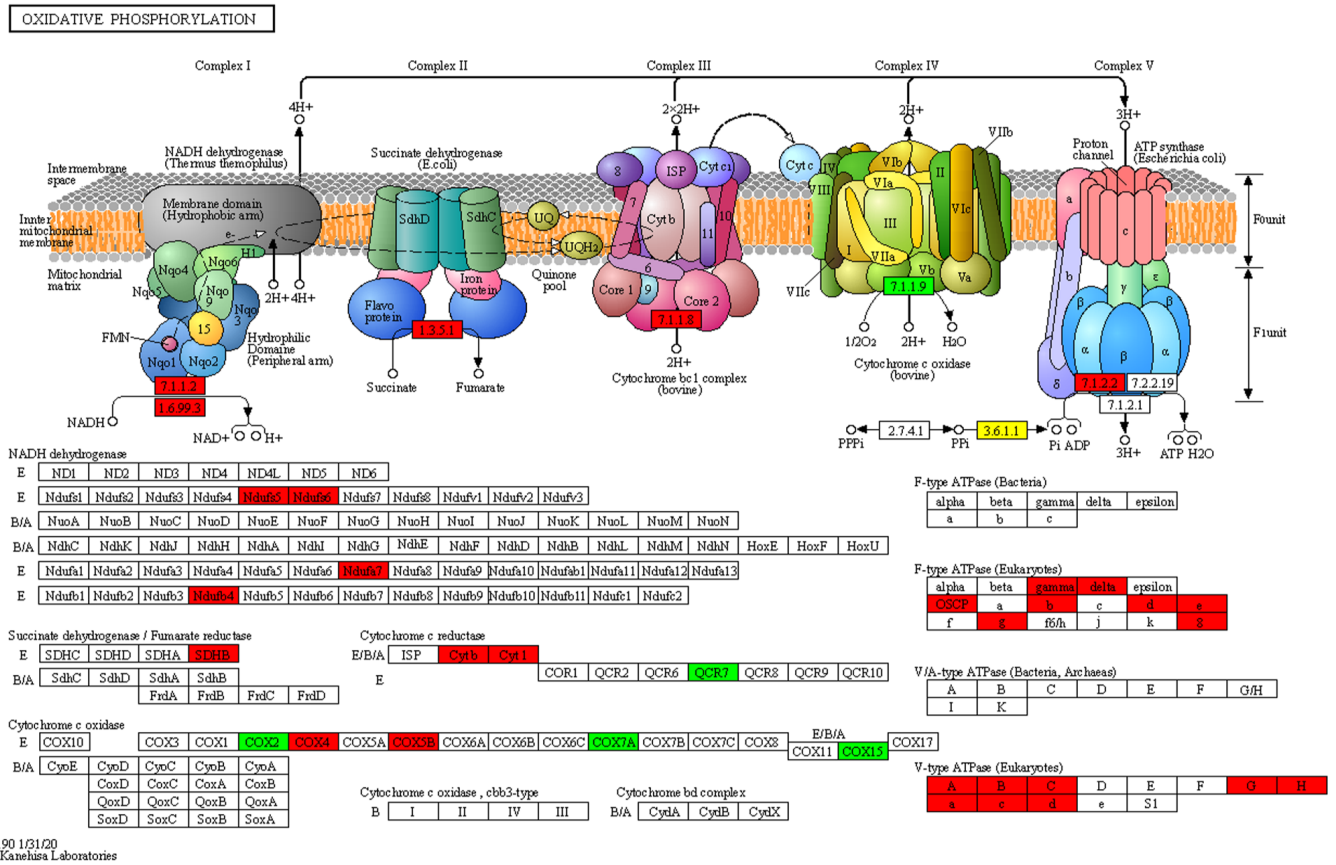


Figure 4. Oxidative phosphorylation pathway cascades. Obtained from the global proteome data by Kyoto Encyclopedia of Genes and Genomes pathway analysis. Red and green squares denote proteins with increased and decreased expression, respectively.

Protein domain enrichment analysis showed that proteins that exhibited increased expression were primarily enriched in domains such as ‘thioredoxin domain’, ‘thioredoxin-like fold’, ‘band 7 domain’, ‘disulfide isomerase’ and ‘mitochondrial carrier domain’ (Fig. 3C). Protein domain enrichment analysis of proteins that showed decreased expression is shown in Fig. S2C, which included ‘GroEL-like apical domain’, ‘GroEL-like equatorial domain’, ‘TCP-1-like chaperonin intermediate domain’ and ‘actin-depolymerising factor homology domain’.

Cluster based on function and characteristics of protein. GO enrichment-based hierarchical clustering analysis of results from GO, KEGG and protein domain functional enrichment revealed that the differentially expressed proteins with P<0.05 were clustered into four groups, Q1 to Q4, based on the ratio of mitochondria derived from MenSCs to SKOV3 cells. Q1 was defined as a ratio between 0.0 and 0.5, which included 583 proteins. Q2 was defined as a ratio between 0.500 and 0.667, which included 173 proteins. Q3 was defined as a ratio between 1.5 and 2.0, which included 137 proteins. Q4 was defined as a ratio >2 and included 592 proteins. In the molecular function category, differentially expressed proteins were primarily associated with ‘ATPase activity, coupled to movement of substances’, ‘GTP binding’ and ‘ATP binding’ (Fig. 5A). ‘Oxoacid metabolic process’, ‘regulation of cell motility’, ‘cellular chemical homeostasis’ and ‘ATP hydrolysis coupled transmembrane transport’ were the subcategories

differentially expressed proteins were most associated with in the biological process category (Fig. 5B). Proteins associated with ‘ribosome’, ‘intrinsic component of organelle’ and ‘proton-transporting two-sector ATPase complex’ were upregulated in cellular component category by enrichment analysis (Fig. 5C).

Differentially expressed protein interaction network. To understand the potential PPIs of the differentially expressed proteins, PPI proteomics network analysis was performed using string. The robust and cross-talking signaling interactions among the top 100 upregulated proteins sorted by P-value are mapped in Fig. S3. STRING 11.5 online software was used for PPI analysis with a confidence score >0.4 (medium confidence). According to this network, proteins associated with OXPHOS and ribosome were significantly enriched.

PRM analysis of differentially expressed proteins. To validate the results from 4D label-free data analysis, PRM was performed on significantly differentially expressed proteins involved in the OXPHOS pathway. Due to limitations associated with low relative abundance, 6 proteins of interest, namely T cell immune regulator 1 (TCIRG1), ATP5PO, ATP6V1B2, ATP5F1C, ATP5PB and ATP5PD, were selected for PRM analysis (Fig. S4). Two unique peptides with anticipated chemical stability were selected for each protein and the relative protein abundance was expressed as the mean of the two normalized peptide peak areas. A total of four (TCIRG1,

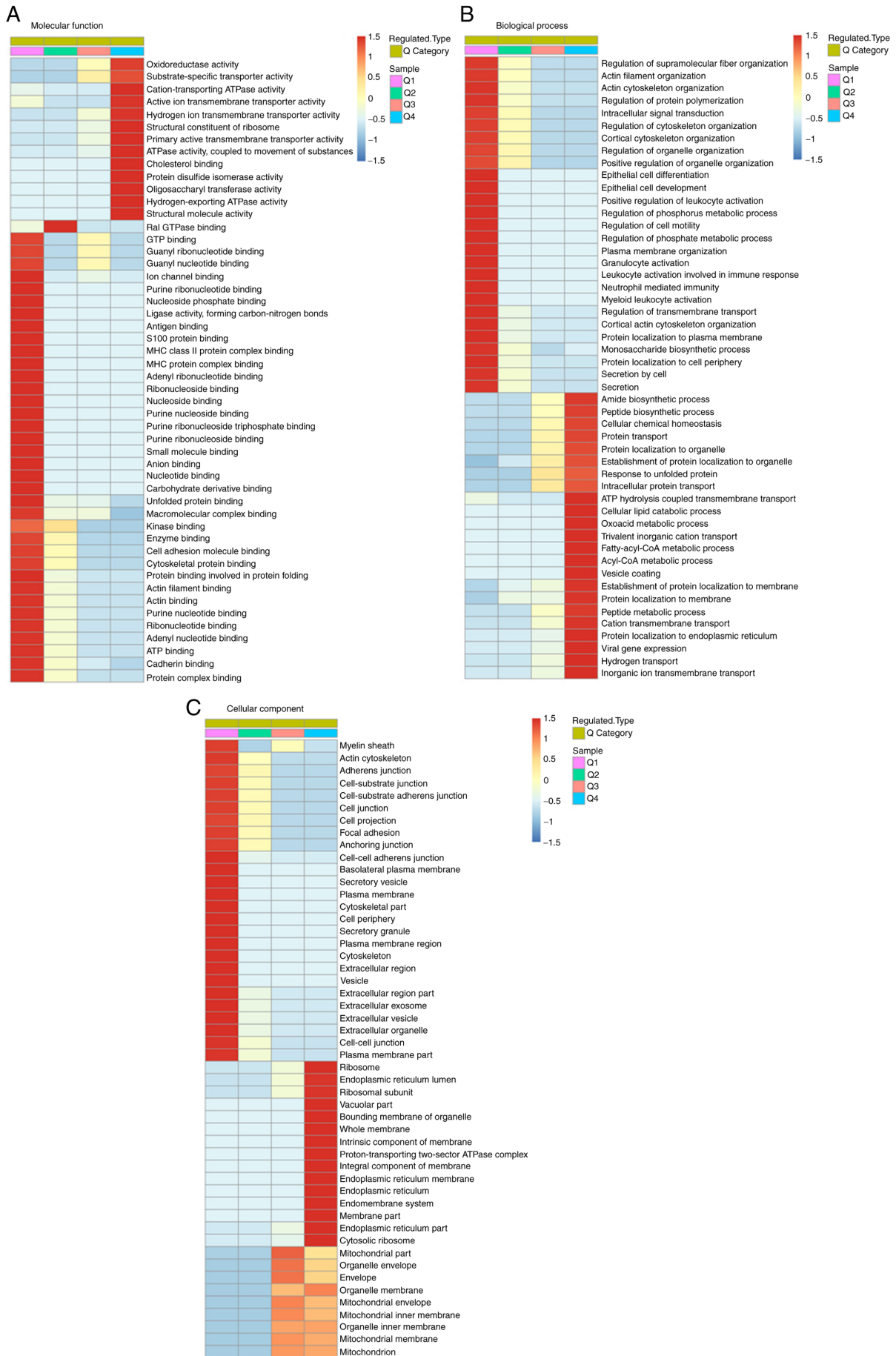


Figure 5. Gene Ontology enrichment-based clustering analysis of the quantified proteins. (A) Molecular function analysis. (B) Biological process analysis. (C) Cellular component analysis.

ATP5PO, ATP6V1B2 and ATP5PD) of the six candidate proteins displayed similar trends to 4D label-free results, which supported the reliability of quantitative proteomics analysis.

Discussion

In the present study, proteomic analysis was performed to identify the differentially expressed proteins between mitochondria derived from MenSCs and the SKOV3 cell line. Subcellular localization of differentially expressed proteins showed that more mitochondrial proteins had increased expression in mitochondria of MenSCs. Functional enrichment analysis revealed that proteins in the OXPHOS pathway were significantly enriched, which was validated by PRM analysis.

Abnormal metabolism is a hallmark of cancer (25). Unlike normal cells, cancer cells depend on aerobic glycolysis to produce the energy needed for rapid proliferation (26). Mitochondrial OXPHOS increases electron leak from the electron-transport chain and mitochondrial superoxide production to stimulate pro-tumoral signaling pathways and antioxidant defenses (27). Increased activity of the OXPHOS pathway has been demonstrated to contribute to cancer metastasis, whereby chemo-resistant cells undergo a shift towards a more active oxidative metabolism (28). In ovarian cancer, increased OXPHOS has been reported to enhance IL-6 production, promoting cancer cell survival and proliferation and impairing responsiveness to chemotherapy (29,30). KEGG pathway enrichment analysis showed that proteins involved in the OXPHOS pathway were significantly enriched in MenSC-derived mitochondria. This indicated that, by facilitating the energy metabolism of the cancer cells, MenSC-derived mitochondria may promote progression of ovarian cancer. Moreover, protein domain analysis showed that 'thioredoxin domain' was significantly enriched. Thioredoxin is a small redox-regulating protein domain that serves key roles in both oxidative stress and hypoxia in the tumoral microenvironment, which is hypothesized to contribute to carcinogenesis (31,32). Therefore, enrichment in 'thioredoxin domain' and 'thioredoxin-like fold domain' in the mitochondria of MenSCs indicated that the transplantation of MenSC-derived mitochondria may enhance ovarian cancer progression.

Therapeutic regimens targeting mitochondria are a potential treatment for cancer in the future (29,33,34). There is *in vivo* and *in vitro* evidence to suggest that mitochondrial transplantation inhibits proliferation of tumor cells or promotes tumor progression (17,35). SCs are optimal donors because of 'high proliferation rate', 'low immunogenicity' and 'low carcinogenicity' to provide mitochondria for transplantation. However, MenSC-derived mitochondria have, to the best of our knowledge, not yet been investigated. By comparing the protein expression profile of the mitochondria from MenSCs and the ovarian cancer cell line SKOV3, it was found that the mitochondria from MenSCs may serve as an enhancer for ovarian cancer.

The present study had limitations. Mitochondria from MenSCs were not transferred into ovarian cancer cells and changes in the biological properties of cancer cells were not observed; experimental results and conclusions were derived from comparative proteomics. Mitochondria derived from

MenSCs were proposed and explored for cancer treatment. The present findings indicated that transfer of mitochondria of MenSCs may promote ovarian cancer progression by activating OXPHOS. Although our hypothesis suggests that transplantation of MenSCs-derived mitochondria into ovarian cancer cells does not inhibit tumor development, previous studies have shown that stem cell-derived mitochondria transplantation is helpful for cancer treatment. This may be related to the source of stem cells, the mode of metastasis, etc. Despite of the promise of cell-free therapy by foreign mitochondria transfer, there is uncertainty regarding SC-derived mitochondrial transplantation and more research is needed in future. In next studies, we will try to select mitochondria or cellular vesicles from other sources of stem cells, transplant them into ovarian cancer cells and explore the status of cancer cells; other research directions also include the selection of mitochondria from MenSCs for the treatment of other malignant tumors.

Acknowledgements

Not applicable.

Funding

The present study was supported by China Postdoctoral Science Foundation Grant (grant no. 2018M641854), National Natural Science Foundation of China (grant no. 81802592), National Natural Science Foundation of China (grant no. 81801402), Natural Science Foundation of Heilongjiang Province (grant no. LH2020H049).

Availability of data and materials

The datasets generated and/or analyzed during the current study are available in the Proteomics Identification Database repository (accession no. PXD036148), ebi.ac.uk/pride/archive/projects/PXD036148.

Authors' contributions

XC and WZ confirm the authenticity of all the raw data. XC, YC and XK designed the study. QK contributed to conception and design. WZ and BL collected menstrual blood samples, extraction of menstrual blood stem cells and their mitochondria and cultured tumor cells. TS and WZ analyzed the data and wrote the manuscript. All authors have read and approved the final manuscript.

Ethics approval and consent to participate

The research proposal for human menstrual blood collection was approved by the Ethics Committee of The Second Affiliated Hospital of Harbin Medical University (approval no. KY2018-105). All volunteers participating in the experiment signed the informed consent.

Patient consent for publication

Not applicable.

Competing interests

The authors declare that they have no competing interests.

References

- Chen L, Qu J, Cheng T, Chen X and Xiang C: Menstrual blood-derived stem cells: Toward therapeutic mechanisms, novel strategies, and future perspectives in the treatment of diseases. *Stem Cell Res Ther* 10: 406, 2019.
- Chen L, Qu J and Xiang C: The multi-functional roles of menstrual blood-derived stem cells in regenerative medicine. *Stem Cell Res Ther* 10: 1, 2019.
- Zhou J, Tan X, Tan Y, Li Q, Ma J and Wang G: Mesenchymal stem cell derived exosomes in cancer progression, metastasis and drug delivery: A comprehensive review. *J Cancer* 9: 3129-3137, 2018.
- Raik S, Kumar A and Bhattacharyya S: Insights into cell-free therapeutic approach: Role of stem cell 'soup-ernatant'. *Biotechnol Appl Biochem* 65: 104-118, 2018.
- Foo JB, Looi QH, Chong PP, Hassan NH, Yeo GEC, Ng CY, Koh B, How CW, Lee SH and Law JX: Comparing the therapeutic potential of stem cells and their secretory products in regenerative medicine. *Stem Cells Int* 2021: 2616807, 2021.
- Huang-Doran I, Zhang CY and Vidal-Puig A: Extracellular vesicles: Novel mediators of cell communication in metabolic disease. *Trends Endocrinol Metab* 28: 3-18, 2017.
- Xu HK, Chen LJ, Zhou SN, Li YF and Xiang C: Multifunctional role of microRNAs in mesenchymal stem cell-derived exosomes in treatment of diseases. *World J Stem Cells* 12: 1276-1294, 2020.
- Parfejevs V, Sagini K, Buss A, Sobolevska K, Llorente A, Riekstina U and Abols A: Adult stem cell-derived extracellular vesicles in cancer treatment: Opportunities and challenges. *Cells* 9: 1171, 2020.
- Liu K, Zhou Z, Pan M and Zhang L: Stem cell-derived mitochondria transplantation: A promising therapy for mitochondrial encephalomyopathy. *CNS Neurosci Ther* 27: 733-742, 2021.
- Nakamura Y, Park JH and Hayakawa K: Therapeutic use of extracellular mitochondria in CNS injury and disease. *Exp Neurol* 324: 113114, 2019.
- Warburg O, Wind F and Negelein E: The metabolism of tumors in the body. *J Gen Physiol* 8: 519-530, 1927.
- Viale A, Corti D and Draetta GF: Tumors and mitochondrial respiration: A neglected connection. *Cancer Res* 75: 3685-3686, 2015.
- Jia D, Lu M, Jung KH, Park JH, Yu L, Onuchic JN, Kaiparettu BA and Levine H: Elucidating cancer metabolic plasticity by coupling gene regulation with metabolic pathways. *Proc Natl Acad Sci U S A* 116: 3909-3918, 2019.
- Permeth-Wey J, Chen YA, Tsai YY, Chen Z, Qu X, Lancaster JM, Stockwell H, Dagne G, Iversen E, Risch H, *et al*: Inherited variants in mitochondrial biogenesis genes may influence epithelial ovarian cancer risk. *Cancer Epidemiol Biomarkers Prev* 20: 1131-1145, 2011.
- Caicedo A, Fritz V, Brondello JM, Ayala M, Dennemont I, Abdellaoui N, de Fraipont F, Moisan A, Prouteau CA, Boukhaddaoui H, *et al*: MitoCeption as a new tool to assess the effects of mesenchymal stem/stromal cell mitochondria on cancer cell metabolism and function. *Sci Rep* 5: 9073, 2015.
- Mombo NB, Gerbal-Chaloin S, Bokus A, Daujat-Chavanieu M, Jorgensen C, Hugnot JP and Vignais ML: MitoCeption: Transferring isolated human msc mitochondria to glioblastoma stem cells. *J Vis Exp* 22: 55245, 2017.
- Gomzikova MO, James V and Rizvanov AA: Mitochondria donation by mesenchymal stem cells: Current understanding and mitochondria transplantation strategies. *Front Cell Dev Biol* 9: 653322, 2021.
- Bray F, Ferlay J, Soerjomataram I, Siegel RL, Torre LA and Jemal A: Global cancer statistics 2018: GLOBOCAN estimates of incidence and mortality worldwide for 36 cancers in 185 countries. *CA Cancer J Clin* 68: 394-424, 2018.
- Signorile A, De Rasmio D, Cormio A, Musicco C, Rossi R, Fortarezza F, Palese LL, Loizzi V, Resta L, Scillitani G, *et al*: Human ovarian cancer tissue exhibits increase of mitochondrial biogenesis and cristae remodeling. *Cancers (Basel)* 11: 1350, 2019.
- Ke X, Li L, Li J, Zheng M and Liu P: Anti-oncogenic PTEN induces ovarian cancer cell senescence by targeting P21. *Cell Biol Int* 46: 118-128, 2022.
- Li F, Wang Y, Li Y, Yang H and Wang H: Quantitative analysis of the global proteome in peripheral blood mononuclear cells from patients with new-onset psoriasis. *Proteomics* 18: e1800003, 2018.
- Lin H, Zhang W, Xu Y, You Z, Zheng M, Liu Z and Li C: 4D label-free quantitative proteomics analysis to screen potential drug targets of Jiangu Granules treatment for postmenopausal osteoporotic rats. *Front Pharmacol* 13: 1052922, 2022.
- Heil LR, Remes PM and MacCoss MJ: Comparison of unit resolution versus high-resolution accurate mass for parallel reaction monitoring. *J Proteome Res* 20: 4435-4442, 2021.
- Dacks JB, Field MC, Buick R, Eme L, Gribaldo S, Roger AJ, Brochier-Armanet C and Devos DP: The changing view of eukaryogenesis-fossils, cells, lineages and how they all come together. *J Cell Sci* 129: 3695-3703, 2016.
- Pavlova NN and Thompson CB: The emerging hallmarks of cancer metabolism. *Cell Metab* 23: 27-47, 2016.
- Vaupel P, Schmidberger H and Mayer A: The Warburg effect: Essential part of metabolic reprogramming and central contributor to cancer progression. *Int J Radiat Biol* 95: 912-919, 2019.
- Payen VL, Zampieri LX, Porporato PE and Sonveaux P: Pro- and antitumor effects of mitochondrial reactive oxygen species. *Cancer Metastasis Rev* 38: 189-203, 2019.
- Zampieri LX, Grasso D, Bouzin C, Brusa D, Rossignol R and Sonveaux P: Mitochondria participate in chemoresistance to cisplatin in human ovarian cancer cells. *Mol Cancer Res* 18: 1379-1391, 2020.
- Emmings E, Mullany S, Chang Z, Landen CN Jr, Linder S and Bazzaro M: Targeting mitochondria for treatment of chemoresistant ovarian cancer. *Int J Mol Sci* 20: 229, 2019.
- Matassa DS, Amoroso MR, Lu H, Avolio R, Arzeni D, Procaccini C, Faicchia D, Maddalena F, Simeon V, Agliarulo I, *et al*: Oxidative metabolism drives inflammation-induced platinum resistance in human ovarian cancer. *Cell Death Differ* 23: 1542-1554, 2016.
- Ghareeb H and Metanis N: The thioredoxin system: A promising target for cancer drug development. *Chemistry* 26: 10175-10184, 2020.
- Karlenius TC and Tonissen KF: Thioredoxin and cancer: A role for thioredoxin in all states of tumor oxygenation. *Cancers (Basel)* 2: 209-232, 2010.
- Pustynnikov S, Costabile F, Beghi S and Facciabene A: Targeting mitochondria in cancer: Current concepts and immunotherapy approaches. *Transl Res* 202: 35-51, 2018.
- Wang J, Li H, Yao Y, Zhao T, Chen YY, Shen YL, Wang LL and Zhu Y: Stem cell-derived mitochondria transplantation: A novel strategy and the challenges for the treatment of tissue injury. *Stem Cell Res Ther* 9: 106, 2018.
- Kheirandish-Rostami M, Roudkenar MH, Jahanian-Najafabadi A, Tomita K, Kuwahara Y, Sato T and Roushandeh AM: Mitochondrial characteristics contribute to proliferation and migration potency of MDA-MB-231 cancer cells and their response to cisplatin treatment. *Life Sci* 244: 117339, 2020.



This work is licensed under a Creative Commons Attribution-NonCommercial-NoDerivatives 4.0 International (CC BY-NC-ND 4.0) License.